Blends of biodegradable poly(butylene adipate-co-terephthalate) with poly(hydroxi amino ether) for packaging applications: Miscibility, rheology and transport properties

Ainara Sangroniz, Leire Sangroniz, Nora Aranburu, Mercedes Fernández, Antxon Santamaria, Marian Iriarte, Agustin Etxeberria*

POLYMAT, Department of Polymer Science and Technology, Faculty of Chemistry, University of the Basque Country UPV/EHU, Paseo Manuel de Lardizabal 3, Donostia 20018, Spain.

* Correspondence to: Agustin Etxeberria (E-mail: agustin.etxeberria@ehu.es)

Abstract

The improvement of the properties of biodegradable poly(butylene adipate-co-terephthalate) (PBAT) through the addition of poly(hydroxi amino ether) (PHAE) is investigated. Analysis by means of DSC, DMTA, FTIR and TEM reveals that blends are partially miscible, with finely dispersed droplet/matrix morphology. Besides of morphology, hydrogen bonds between both, hydroxyl groups and tertiary amines in neat poly(hydroxi amino ether), and with carbonyl groups of poly(butylene adipate-co-terephthalate) in the blends, work out the linear viscoelastic properties and the time relaxation spectrum. Blends rich in poly(hydroxi amino ether) show the highest relaxation times and consequent strain hardening behaviour, which facilitates film elaboration for packaging.

Permeability to water vapour, limonene and carbon dioxide is measured obtaining a great reduction on PBAT permeability with the addition of poly(hydroxi amino ether), specially for carbon dioxide. The mechanical properties of the blends are similar to the polymer that forms the matrix. Overall, this work aims to shed light on the effect of a second component on the properties of a biodegradable polymer in order to design suitable materials for packaging applications.

Keywords: Polymer blends; biodegradable polymer; miscibility; rheology; transport properties; packaging

Introduction

Biodegradable polymers have attracted a great attention over the last years, due to the growing awareness of the environmental problems associated to the huge volume of polymer waste. Nowadays, the employed polymers for packaging applications have a short service life and they are not degradable. Biodegradable polymers offer a potential solution, notwithstanding they have, in general, low barrier character to gases and vapours and poor mechanical properties. Therefore, polymer blending is a widely employed method in order to improve their properties [1-3].

Poly(butylene-adipate-co-terephthalate) (PBAT), generally known under the tradename of Ecoflex^{R}, is an aliphatic aromatic copolyester that can be fully degraded in few weeks [4]. It has good mechanical properties, such as adequate toughness and tear resistance, but it has a low barrier character to water vapour, oxygen and carbon dioxide [2]. In order to improve the properties of PBAT different approaches have been carried out being one of them blending with another polymer, for example poly(hydroxy ether of bisphenol A), which presents an outstanding barrier character, and that leads to miscible blends [5].

Poly(hydroxi amino ether) (Blox^{R}, PHAE), which has a similar characteristic to phenoxy, is a good candidate to improve the limitations of PBAT, since it presents an outstanding barrier quality to oxygen and carbon dioxide. It combines the great adhesion and durability of epoxy thermoset resins, with the processability of thermoplastics. It contains hydroxyl groups that can form strong specific interaction via hydrogen bonds, which leads to compatible blends [6-8]. Poly(hydroxi amino ether) polymer have been found to be partially miscible with polyamide-6 [9, 10], poly(butylene terephthalate) [11], poly(ethylene terephthalate) [12] and poly(caprolactone) [13].

Since PBAT/PHAE blends are potential candidates for packaging industry, and films are obtained usually by blow extrusion, the rheological properties under shear and extensional flow must be investigated. The rheological features of immiscible blends depend on the concentration of each polymer phase, type of flow field, interaction between phases, morphology and interfacial tension between phases [14, 15]. In the literature the relationship between rheology and morphology has been widely investigated [14, 16, 17]. It has been proved that the measurements performed in the linear viscoelastic regime are able to detect small differences in the morphology

due to the coalescence of the droplets [18]. Some authors have tried to relate the morphology of immiscible blends with different rheological plots, like relaxation spectrum and others, with only a relative success [19, 20]. Regarding the rheological properties under extensional flow, most of the works focus on the study of polyolefins, although there are a few studies on biodegradable polymers. For instance, the extensional flow of PLA has been studied [21-23].

In the packaging sector the characterization of the transport properties is a necessary task. Depending on the characteristic of the packed product different permeability to penetrants is required. For example, fruits and vegetables need oxygen for respiration whereas in other products oxygen can provoke the growth of microorganism and the oxidation of fats. In literature the transport properties of biodegradable polymers, such as polylactide, poly(caprolactone) and poly(hydroxybutyrate), have been widely studied [24-26]. Taking into account that in general biodegradable polymer present poor barrier character different methods have been used to improve this property: blending with another polymer or adding different fillers [27, 28]. In the case of immiscible polymer blends the morphology also affects the transport properties [29, 30].

In this work PBAT/PHAE blends are studied. Miscibility is analysed by means of Differential Scanning Calorimetry (DSC), Infrared Spectroscopy (FTIR), Dynamic Mechanical Thermal Analysis (DMTA) and Transmission Electron Microscopy (TEM). Rheological properties under shear flow, in the linear viscoelastic regime, and under extensional flow are studied and linked to the morphology of the blends and the presence of hydrogen bonds. Finally the mechanical performance and the permeability to water vapour, limonene and carbon dioxide is measured to assess the suitability of these blends for packaging applications.

Experimental part

Materials

Poly(butylene adipate-co-terephthalate) (PBAT) of a molecular weight Mw = 75000 g/mole, known as Ecoflex^{R}, was purchased from Basf (Ecoflex F Blend C1200). PBAT is a random copolymer with adipate/terephthalate ratio of 47/53 in mole. The poly(hydroxi amino ether) resin (PHAE) of MFI = 8.5 g/10 min at 200 °C and 2.16 kg load ASTM D-1238 was supplied by Dow Chemical, under the trade

name Blox^{R}. The respective Newtonian viscosities of PBAT and PHAE, obtained as explained below in the corresponding sections, are 800 and 40000 Pa s.

Blend preparation

PBAT/PHAE blends were prepared in the molten state employing a Model CS-183 MMX mixer at 190 °C and 40 rpm. Films for permeability measurements with thickness of 60 μm and 200 μm were obtained by hot pressing using a Graseby Specac device at 190 °C. Sheets of 1 mm thickness for rheological measurements were obtained also at 190 °C by compression moulding. The membranes and sheets were dried in vacuum 2 days at 70 °C and at least 5 days at room temperature.

Differential Scanning Calorimetry (DSC)

Thermal properties were measured in a differential scanning calorimeter model Q2000 V24 TA Instruments. Samples of approximately 5 mg were encapsulated in aluminium pans and two scans were performed from -80 °C to 200 °C at 10 °C/min heating and cooling rate.

Thermo-mechanical properties

Dynamic mechanical thermal analysis was performed using a Triton 2000 DMA (Triton Technology, Ltd.) in bending mode from -55 to 120 °C. The measurements were performed with a heating rate of 4 °C/min and a frequency of 1 Hz, which are commonly used to evaluate the glass transition temperature T_g.

Infrared spectroscopy

The infrared spectra were recorded in a FTIR spectrometer Nicolet Magna 560 using an ATR unit Golden Gate. The spectra were recorded with 2 cm^{-1} resolution.

Thermogravimetric analysis (TGA)

Thermal gravimetric analysis was performed using a TGA Q500 (TA Instruments) equipment. Samples of 3-5 mg were prepared and heated from room temperature to 800 °C at 10 °C/min heating rate under nitrogen flux of 100 mL/min.

Morphological characterization (TEM)

Morphological characterization was carried out employing a TECNAI G2 20 TWIN (FEI) transmission electron microscopy (TEM) with an acceleration voltage of 200 keV. The samples were cut at -50 °C using a LEICA EMFC6.

Rheological measurements

Rheological measurements were carried out using an ARG-2 rheometer (TA Instruments). Small amplitude oscillatory shear measurements were conducted under nitrogen atmosphere at 150 °C using a parallel plates geometry (diameter 25 mm). Frequency sweeps were carried out in the linear viscoelastic regime from 628 to 0.05 rad/s.

The rheological properties under uniaxial extensional flow were measured using the Extensional Viscosity Fixture (EVF) of an ARES rheometer (TA Instruments) at 150 °C.

Mechanical measurements

The mechanical properties were measured employing an Instron 5565 testing machine at a crosshead displacement rate of 5 mm/min and 22 °C. The films have a thickness between 100-150 μm and the specimens were cut according to ASTM D638 type V. At least 5 specimens were tested for each reported value.

Permeability measurements

Water vapour and limonene transmission rate were measured in a permeation cell at 25 °C according to ASTM E96–95 method. The cell is a small container made of polytetrafluoroethylene, which is partially filled with water or limonene and a polymeric membrane in the top. The measurements were carried out in a Sartorius BP 210 D balance with 10^{-5} g readability and the mass loss was recorded in a computer [31]. The values shown are the average of at least 5 measurements.

Carbon dioxide permeability was measured in a permeation cell built in our laboratory, which is similar to other equipments described in literature [32-34]. The measurements were carried out at 1 atm and 25 °C and the values shown are the average of at least 5 measurements.

Results and Discussion

Analysis of miscibility

From a practical point of view, miscibility of the polymer blends is usually determined analysing the glass transition temperature and considering that for blends with a single glass transition temperature miscibility is achieved, whereas blends that show two glass transition temperatures are immiscible [35].

The thermal properties of PBAT/PHAE blends are reported in Table 1 (See thermograms in Figure S1 of supplementary information). The melting temperature and degree of crystallinity were evaluated from the first heating scan. The glass transition temperatures were determined by Dynamic Mechanical Thermal Analysis (DMTA), as explained below.

Poly(butylene adipate-co-terephthalate) shows three melting peaks at 47.2 °C, corresponding to adipate sequence, and 89.3 and 121.0 °C, corresponding to PBT sequence [4]. In literature X ray measurements show that the diffraction pattern of PBAT resembles that of poly(butylene terephthalate) (PBT), with some adipate units as impurities [4]. The observed two melting peaks in the DSC thermogram for PBT can be attributed to two crystalline structures: α and β form, which undergo melting-recrystallization process during heating [36]. In order to calculate crystallinity $\Delta H_m^0 = 142\,J/g$ is considered for PBT [37] and $\Delta H_m^0 = 135\,J/g$ for PBA [38]. Our DSC results indicated a crystallinity of 14 % for PBAT, which is in accordance with the previous data reported in literature [4].

The addition of PHAE decreases the melting temperature of the peak located near 89 °C, due to the formation of less perfect crystals. This is an usual behaviour in miscible or partially miscible blends [39]. The second melting peak increases slightly with PHAE content, but the change is very subtle. In the case of 25 PBAT/75 PHAE blend, a broad small peak located at 105.1 °C is observed, due to the overlap of the aforementioned two melting peaks of PBAT.

The blend containing 25 % PHAE has a similar crystallinity compared to neat PBAT whereas the addition of 50 % PHAE decreases the crystallinity degree, indicating that the second component hinders the crystallization of PBAT. However, for the blend containing 75 % PHAE the crystallinity level is much higher than that of pure PBAT, showing again the peculiarity of this blend.

Table 1. Thermal properties of PBAT/PHAE blends, as determined by DSC and DMTA.

Sample	T_g (ºC) (DMTA)	T_m (°C)	X_c (%)	$X_{c\,PBAT}$ (%)
PBAT	-20	47.2[a], 89.3[b], 121.0[c]	14	14
88 PBAT/12 PHAE	-20, 75	48.1[a], 80.7[b], 127.2[c]	15	17
75 PBAT/25 PHAE	-18, 82	83.9[b], 121.8[c]	9	13
63 PBAT/37 PHAE	-18, 81	47.4[a], 79.7[b], 125.6[c]	9	14
50 PBAT/50 PHAE	-18, 83	88.2[b], 122.6[c]	3	5
38 PBAT/62 PHAE	-20, 71	81.0[b], 122.6[c]	6	15
25 PBAT/75 PHAE	-24, 88	105.1	6	22
13 PBAT/87 PHAE	*, 87	129.5	1	5
PHAE	91	-	-	

* The transition which corresponds to PBAT phase was not properly detected. [a,b,c] correspond to the different melting peaks labelled in the Figure S1.

To gain insight on the phase behaviour of the blends, DMTA measurements were carried out. The measurements are shown in Figure 1, where not all the blends are shown for the sake of clarity (see Supporting Information, S2) and the maximum of tan δ corresponds to the glass transition temperature. The values of the glass transitions temperatures obtained by DMTA are included in Table 1. The glass transition temperature of PBAT appears at -20 ºC and that of PHAE at 91 °C, both values being higher than those obtained by DSC, which are, respectively, -27 ºC and 77 ºC. The observed values for the pure polymers are similar to those found in the literature [40, 41]. In the case of PHAE, a small and broad peak is observed near -40 °C attributed to a secondary transition [6]. This low temperature relaxation cannot be detected by DSC, indicating that, in this case, DMTA is a more sensitive technique.

For the blends, the respective glass transition temperatures, corresponding to PBAT and PHAE fractions, are displaced from those of neat polymers which suggest

that the blends are partially miscible. As detected by DMTA, the glass transition temperature of PBAT phase is increased for blends containing 25 and 50 % of PHAE. For 25 PBAT/75 PHAE blend the T_g corresponding to PBAT phase is lower than that of neat PBAT. In literature this behaviour has been attributed to the differences of the thermal expansion coefficients of the dispersed phase and the matrix. This would lead to a thermal stress and the soft phase would be eventually dilated [42, 43]. However, Granado et al. observed a similar result for poly(propylene)/PHAE blends [44] and they attributed the glass transition temperature reduction to the migration of a low molecular additive present in PHAE, which acts as a plasticizer. They corroborated this result by means of Size Exclusion Chromatography SEC/GPC analysis [44]. Considering that both hypotheses are acceptable for our blends, currently we have not a definitive explanation for the T_g corresponding to PBAT phase being lower than that of neat PBAT.

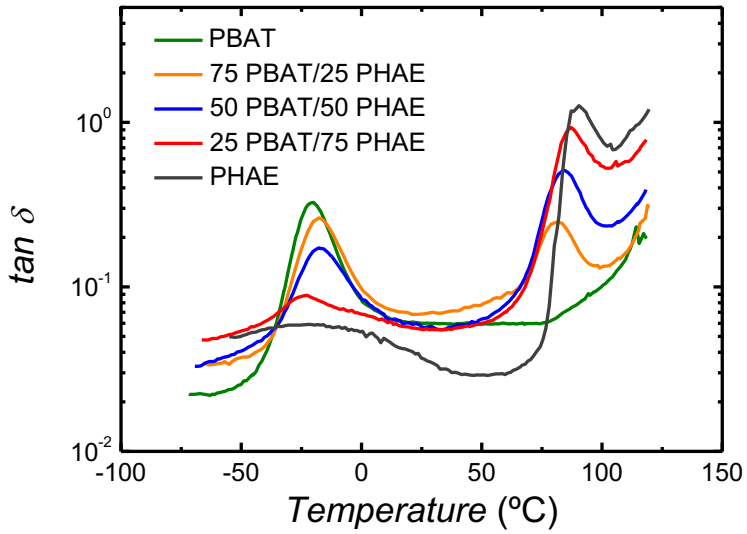

Figure 1. Tan δ vs temperature of PBAT/PHAE blends and pure polymers.

Infrared spectroscopy is a very useful technique to characterize qualitatively the miscibility of polymer blends through the analysis of the interactions between polymers [45]. Figure 2 shows the carbonyl stretching band of PBAT and PBAT/PHAE blends.

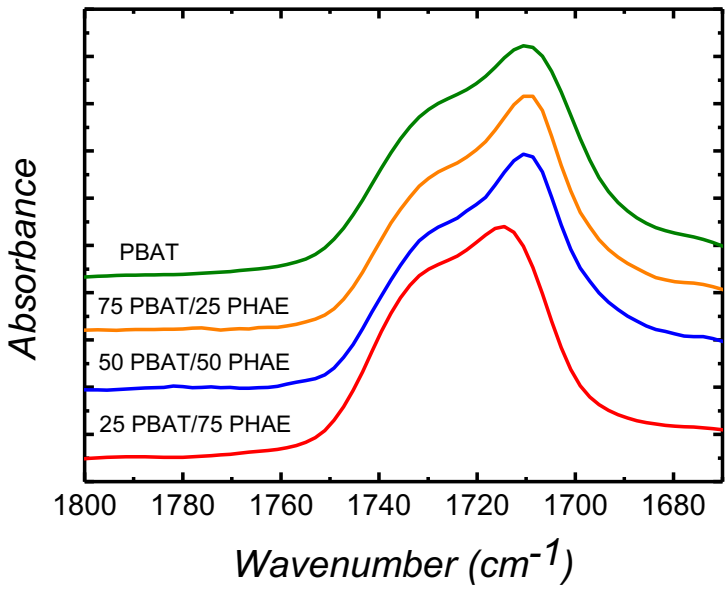

Figure 2. Carbonyl stretching band of PBAT and PBAT/ PHAE blends.

PBAT shows a band located at 1709 cm^{-1} and a shoulder at 1730 cm^{-1} corresponding to the bands of the crystalline and amorphous phase, respectively. For 75 PBAT/25 PHAE and 50 PBAT/50 PHAE blends the bands are almost identical. But, for 25 PBAT/75 PHAE blend the band which corresponds to the amorphous fraction is shifted to 1715 cm^{-1}, whereas for neat PBAT it appears at 1709 cm^{-1}. This shift is related to the hydrogen bonding associations brought about by the hydroxyl and tertiary amine groups of poly(hydroxi amino ether) (PHAE), see Scheme 1 for the structures of the interactions. Similar results have been observed in literature for an immiscible polyester/polyether blend [46].

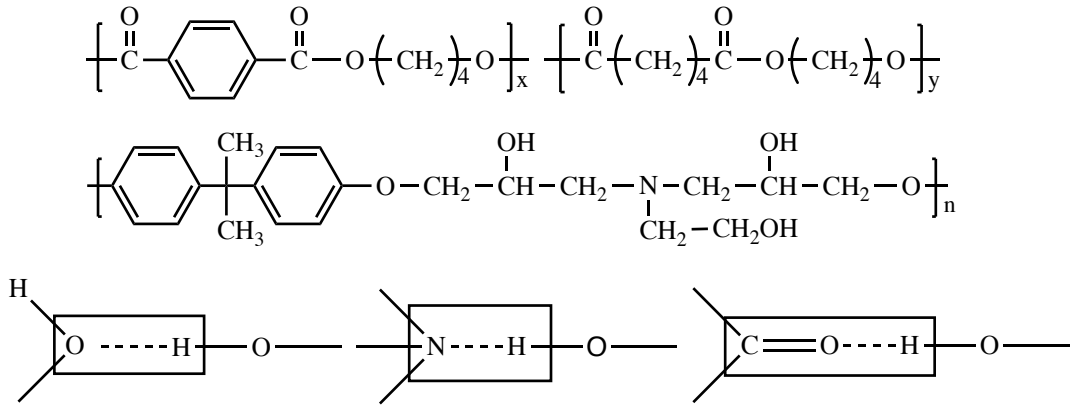

Scheme 1. Structures of PBAT and PHAE and the possible intramolecular interactions in PHAE and intermolecular interaction between PBAT and PHAE.

Figure 3 shows the thermogravimetric traces obtained for PBAT/PHAE blends, for the values corresponding to 5 % and 50 % of the weight loss, see Table S1 in supplementary information. Both, PBAT and PHAE have a similar thermal stability with $T_{\%5}$ = 331.4 °C and 324.6 °C values, respectively. All the blends are less stable than the neat components, being 25 PBAT/75 PHAE composition the least stable.

From the collected data it is clear that the components influence each other destabilizing the blend, being the destabilization more severe for the blends rich in PHAE. Similar results were obtained by Eguiazabal and Iruin [47] for blends of poly(hydroxyl ether of Bisphenol A), which is similar to PHAE, and different polyesters.

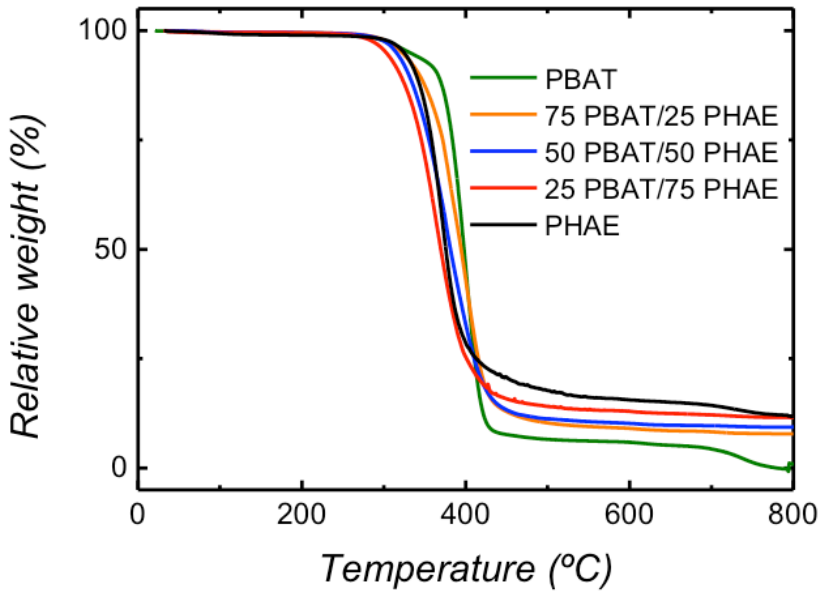

Figure 3. Thermogravimetric traces of PBAT/PHAE blends.

In order to analyse the morphology of the blends micrographs were obtained by transmission electron microscopy. As can be seen in Figure 4 all the blends exhibit droplet/matrix morphology. For the central composition 50 PBAT/50 PHAE a cocontinuous morphology could be initially expected. However, this is not observed, because the viscosity of PBAT is much lower than that of PHAE (see below) compelling the latter to form a dispersed phase in the PBAT continuous phase.

The droplets are homogeneously distributed in the matrix and the obtained morphologies are similar to that observed for poly(caprolactone)/PHAE and

poly(butylene terephthalate)/PHAE blends, in which small particles are also found [13, 40].

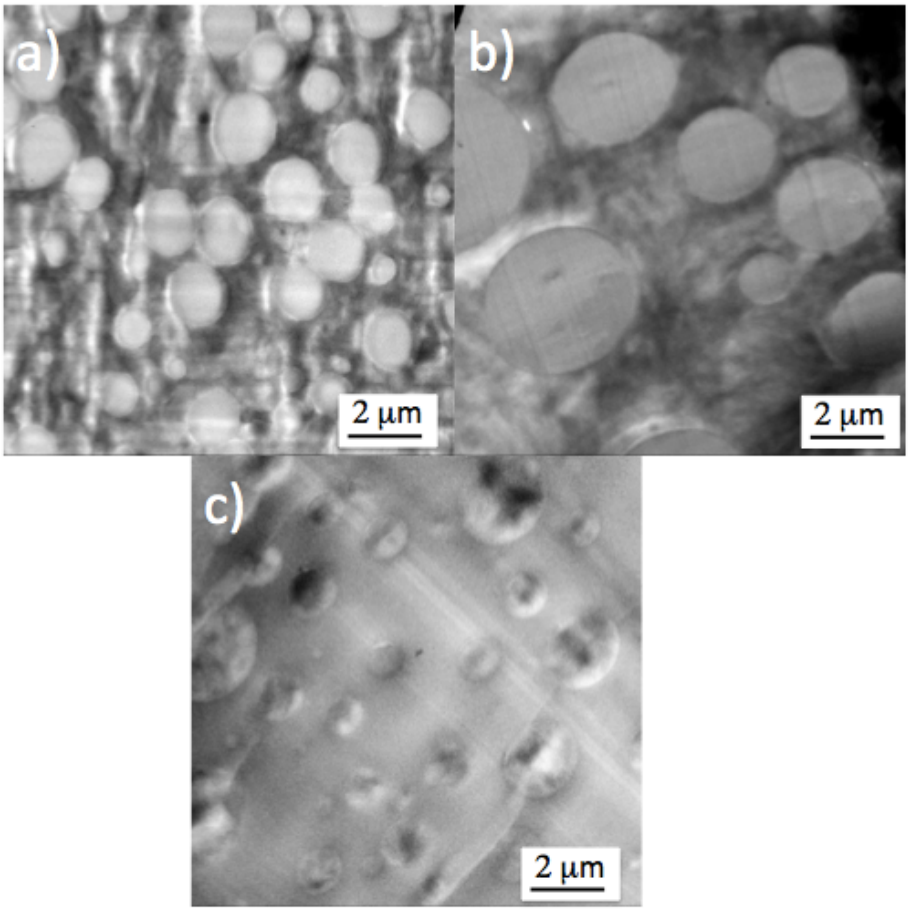

Figure 4. TEM micrographs of cryofractured surfaces of (a) 75 PBAT/25 PHAE (b) 50 PBAT/50 PHAE and (c) 25 PBAT/75 PHAE.

The number average diameter (d_n), volume average diameter (d_v) and polydispersity (D) of the blends were calculated using the following equations and the corresponding values are reported in Table 2. For the histograms see Figure S3 and S4 in Supporting Information.

$$d_n = \frac{\sum n_i d_i}{\sum n_i d_i} \quad (1)$$

$$d_v = \frac{\sum n_i d_i^4}{\sum n_i d_i^3} \quad (2)$$

$$D = \frac{d_v}{d_n} \quad (3)$$

Table 2. Average diameter in number and volume and polydispersity for PBAT/PHAE blends.

	d_n (μm)	d_v (μm)	D
75 PBAT/25 PHAE	0.69	0.87	1.3
50 PBAT/50 PHAE	1.0	1.4	1.3
25 PBAT/75 PHAE	0.39	0.59	1.5

The number average diameters of the dispersed phase are: 0.69 μm for 75 PBAT/25 PHAE, 1.0 μm for 50 PBAT/50 PHAE and 0.39 μm for 25 PBAT/75 PHAE. For the blend which contains up to 50 % PBAT the polymer that forms the matrix is PBAT, whereas for 75 PBAT/25 PHAE blend the polymer forming the matrix is PHAE.

Density measurements

The density of PBAT/PHAE blends has been characterized since it could give an approximate estimation about the variation of the free volume with the composition of the blends. As it can be observed in Table 3 the density values vary slightly with the composition. The density values change with composition following the simple additivity rule, except the blend 50 PBAT/50 PHAE which presents a density value that deviates negatively from additivity. Therefore, it could be deduced that samples have even smaller excess free volume. Taking into account the densities of pure polymers, the volume fraction is practically identical to weight fraction one: 74.7 % PBAT, 49.6 % PBAT and 24.7 % PBAT.

Table 3. Density values for PBAT/PHAE blends.

Sample	Density (g/cm^3)
PBAT	1.2258
75 PBAT/25 PHAE	1.2209
50 PBAT/50 PHAE	1.2139
25 PBAT/75 PHAE	1.2108
PHAE	1.2058

Rheology

Small amplitude oscillatory shear measurements (SAOS)

Dynamic rheological measurements in the linear viscoelastic regime have been carried out, this kind of measurements are very useful to characterize polymer blends since they are sensible to the morphology, the interfacial tension and the composition of the blend [14, 15].

Figure 5 shows the elastic modulus against frequency for the homopolymers and blends. The homopolymers exhibit a behaviour close to that offered by the general linear viscoelastic model [48], characterized by the scaling law $G' \propto w^2$ with a slope of 2 in log-log plots. However, the blends deviate from this feature, due to the elasticity resulting from the interfacial tension between the two phases. Differing from the other samples, 25 PBAT/75 PHAE blend shows a trend to a plateau at low frequencies. This plateau is observed in literature typically for sufficiently concentrated polymer suspensions, for instance percolated polymer nanocomposites [49, 50] and polymer gels [48, 51-53], rather than in emulsions. Our inceptive results can be due to an effect of the observed very small droplets size (volume average diameter of 0.59 μm), which enhances the interfacial stress and so the elastic modulus.

A viscoelastic model for emulsion-like blends was proposed by Palierne [54] contemplating the morphology, the behavior of the two phases, and the interfacial tension between them. This model represents actually a crucial advance with respect to the Kerner model [55] which only considers the composition effect and is rather valid at high frequencies, where the effect of the interfacial tension is not significant.

A good fitting of the dynamic viscoelastic moduli to Palierne´s model requires that the elastic moduli of the polymers differ in less than one order of magnitude. Unfortunatelly, this condition is not fufiled for our PBAT and PHAE polymers, as can be seen in Figure 5, and, therefore, the use of Palierne's model was fruitless in our case.

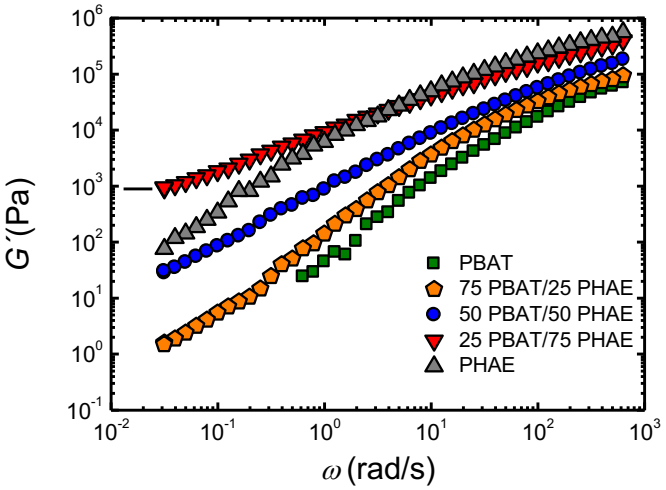

Figure 5. Storage modulus vs frequency for the homopolymers and the blends. The line in 25 PBAT/75 PHAE sample is to guide the eye.

At low frequencies, where the viscoelastic behaviour is controlled by interfacial and morphological effects, SAOS data, like those of Figure 5, allow calculating the relaxation spectrum of each sample, using the following equations [56, 57],

$$G'(\omega) = \int_{-\infty}^{\infty} H(\lambda) \frac{\omega^2 \lambda^2}{1+\omega^2 \lambda^2} d\ln\lambda \quad (4)$$

$$G''(\omega) = \int_{-\infty}^{\infty} H(\lambda) \frac{\omega\lambda}{1+\omega^2 \lambda^2} d\ln\lambda \quad (5)$$

where $H(\lambda)$ is the relaxation spectrum and λ is the relaxation time. The results are shown in Figure 6. As can be seen, PBAT and PHAE show, respectively, only one relaxation peak. For PBAT the peak relaxation time is 0.016 s, which is shorter than that obtained in literature for the same polymer grade by Carreau et al. [18], 0.8 s. Also a value of 0.5 s was obtained for PBAT, with a lower molecular weight than our sample, by Al Itry et al. [21]. For PHAE polymer the relaxation time at the peak is 0.58 s. The shoulder visible at approximately 0.05 s may be explained by the relaxation of the aliphatic part of the PHAE which relaxes faster than the segments that are near the bulky aromatic groups. The relative high relaxation times of this polymer are due to the formation of hydrogen bonds between the tertiary amine and hydroxyl groups. It has been reported that, in general, hydrogen bonds broaden the relaxation time spectrum towards long times [58, 59]. As far as we know this is the first reported information on the relaxation times of a poly(hydroxi amino ether).

The blend rich in PBAT, 75 PBAT/25 PHAE, shows only one relaxation peak at 0.05 s, which can be due to the small amount of PHAE or to its high viscosity, with respect to the viscosity of PBAT, as it is discussed below. This indicates that PHAE droplets do not deform substantially, which is compatible with the invisibility of the relaxation peak of this polymer, as has been reported previously in literature for PMMA/PS and mLLDPE/LDPE [60-62].

For 50 PBAT/50 PHAE and 25 PBAT/75 PHAE blends, two peaks can be distinguished, respectively: at 0.15 s and 2 s for 50 PBAT/50 PHAE and 0.02 s and 3 s for 25 PBAT/75 PHAE. Logically, the peak at the lowest relaxation time is attributed to the relaxation of PBAT phase, whereas the second one is related to the relaxation of PHAE phase and the form relaxation of the droplets. In literature, polylactide/poly(butylene adipate-co-terephthalate) and polylactide/poly(butylene succinate-co-adipate) immiscible blends have been investigated [18] and in both cases two relaxation peaks were detected. One of the peaks was related to the relaxation of the matrix, and the other to the shape relaxation of the droplets. If the relaxation time of the different blends is analysed it can be seen that the presence of PHAE shifts the relaxation peak of PBAT to longer times; the same occurs in the case of PHAE peak in presence of PBAT. Therefore the presence of other phase hinders the relaxation process, giving rise to longer relaxation times.

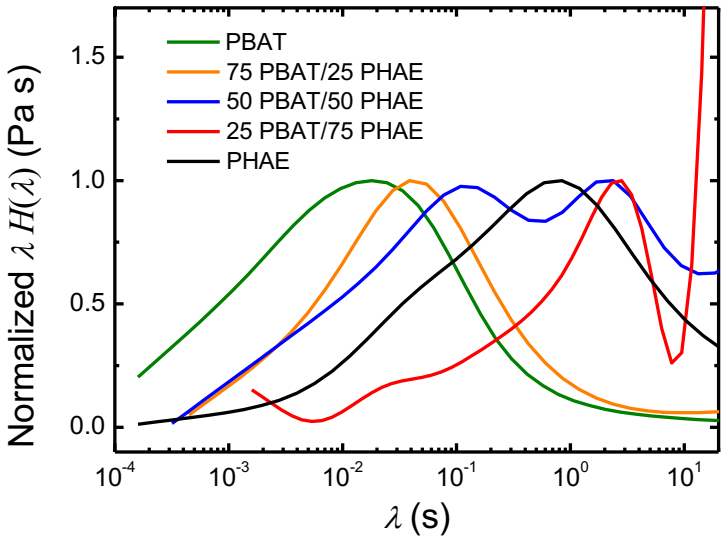

Figure 6. Normalized time weighted spectra for all the systems studied.

In Figure 7 the absolute value of the complex viscosity against frequency is shown. As expected, homopolymers exhibit a Newtonian behaviour al low frequencies, followed by a viscosity decrease as frequency is increased. This is concomitant with the pseudoplastic or shear thinning behaviour, observed in steady state continuous flow, characterized by a viscosity decrease as shear rate is increased. When the so called Cox Merz rule [63] is fulfilled, complex viscosity and steady state viscosity coincide at equivalent frequencies and shear rates. This fulfilment has not proven in our case, because continuous flow tests have not been contemplated. The blend rich in PBAT, 75 PBAT/25 PHAE, shows the same response. Moreover, the complex viscosity values of the former lie close to those of pure PBAT, which indicates that the matrix governs the viscoelastic properties of this blend, as is deduced from relaxation time spectrum results (Figure 6). However, for the blends of the highest PHAE concentration 25 PBAT/75 PHAE a viscoplastic behaviour is obtained, characterized by a continuous increase of the viscosity as the frequency is decreased.

This behaviour arises from the interfacial tension between the phases, which brings about an increase of the elastic component of the complex viscosity $\eta'' = G'/w$. The decrease of the viscosity with frequency is more patent when comparing the viscosity results of PHAE to those of 25 PBAT/75 PHAE blend. It can be stated that the matrix, PHAE polymer, governs the complex viscosity. But, it should be remarked that the very small droplets of PBAT (volume average diameter of 0.59 μm) give rise to a high interfacial surface, that leads to the increase of the complex viscosity in the region of low frequencies.

In general terms, it can be said that the viscous behaviour observed in blends at low frequencies reflects the influence of phase interactions [14]. In a different way, the results of the complex viscosity at high frequencies catch the expected resistance to flow during processing. In this sense, the observed low viscosity of 25 PBAT/75 PHAE blend at high frequencies allows envisaging a good processability for this blend.

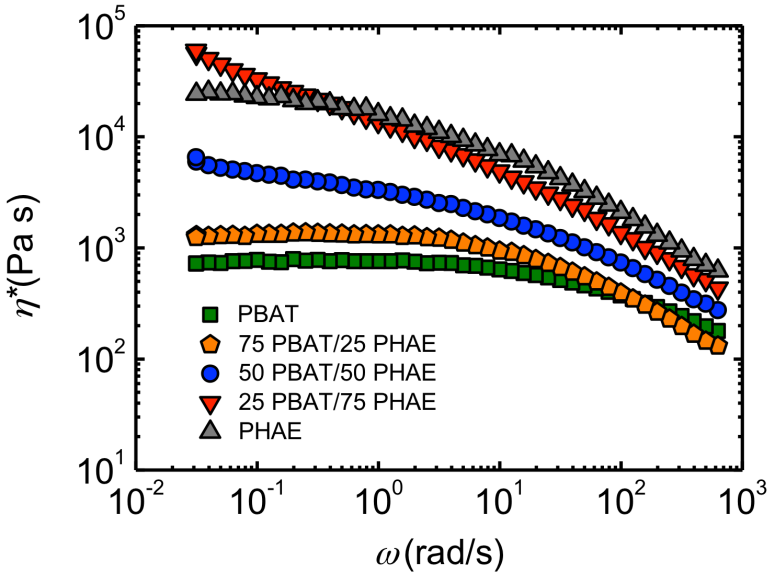

Figure 7. Dynamic viscosity as a function of frequency for the different systems studied.

The so called Van Gurp – Palmen or Mavridis-Shroff plots (VPMS) [64-66], which consist in representing the phase angle δ as a function of the complex modulus G^*, have been used to characterize polymer blends [19, 20, 67, 68]. For instance, Macosco et al. [20] have tried to relate the morphology of polystyrene/styrene-ran-acrylonitrile copolymer immiscible blends with the shape of VPMS plots.

In Figure 8 plots of the phase angle δ as a function of the complex modulus G^* are presented. Phase angle brings about an idea of the viscoelastic nature of the material because for liquids δ is near 90 º whereas for solids the phase angle is near 0 °. Both pure polymers, PBAT and PHAE, as well as the blend with the highest PBAT concentration, 75 PBAT/25 PHAE blend, show the behaviour observed for an homogeneous melt, that is to say a trend to a constant δ value (close to 90 º) at low G^* values and a decrease towards the entanglement plateau modulus in the right side of the plot. It can be said that VPMS plots are not able to detect the presence of the PHAE phase in 75 PBAT/25 PHAE blend, which can be due to the wrapping effect of the much less viscous PBAT phase. Actually, it is known that that the less viscous phase tends always to encircle the more viscous phase. The very high viscosity ratio, 50, of the blend masks the eventual effect of the interfacial tension at low frequencies. 50 PBAT/50 PHAE blend shows a lower δ□ below 80 degrees, as G^* tends to zero, which reflects an increase of the elasticity compatible with the droplets/matrix

morphology shown in Figure 4. This effect is more patent for 25 PBAT/75 PHAE blend, which shows an inflection at low G^* values, i.e. at low frequencies, similar to that reported in the literature for PP/PA blends [68] and attributed to the shape relaxation of the corresponding droplets.

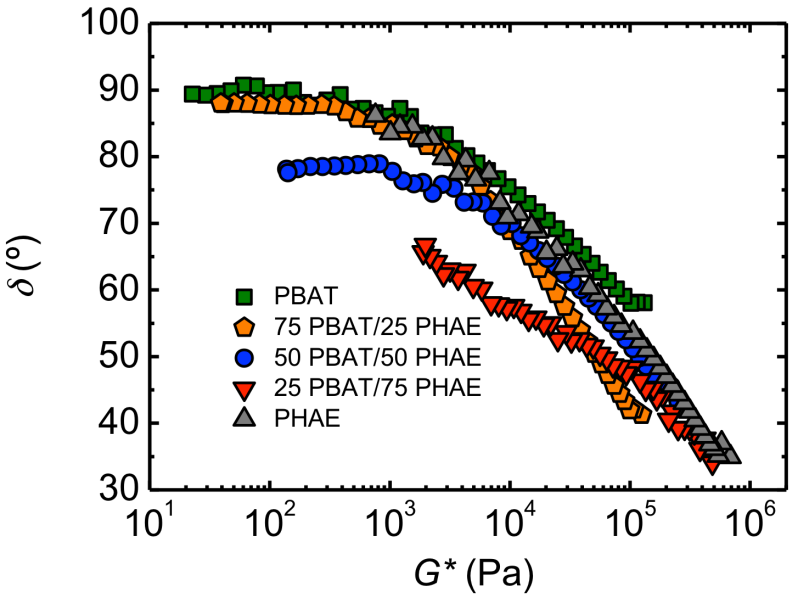

Figure 8. Van Gurp – Palmen- Mavridis-Shroff plots (delta vs complex modulus) for the different systems.

Extensional flow

In Figure 9 the transient extensional viscosity of both homopolymers is presented, as a reference for the results of the blends, which are in turn presented in Figure 10. Pure PBAT shows a strain softening behaviour, that is to say a concave increase of the viscosity towards a constant value, although it contains long chain branches which usually result in strain hardening. On the contrary, PHAE polymer displays a strain hardening response characterized by a convex increase of the viscosity at long times. PBAT, which is a long branched polymer, should be in principle more prone to strain hardening than a linear polymer like PHAE, because strain hardening has been reported in a number of long branched polymers [69, 70]. But, actually, strain softening has been observed in the literature for PBAT at 180 ºC [21]. This confirms that long chain branching itself does not bring about strain hardening. Moreover, strain hardening has been observed in linear PS and

poly(butadiene) samples, as reported in the literature [69, 71]. The lines in Figure 9 represent the Trouton law [14], which states that extensional viscosity is 3 times the Newtonian viscosity obtained under shear flow, $\eta_e=3\eta_o$. Therefore, applying this law requires knowing the Newtonian viscosity of the sample, which in our case is only possible for PBTA and PHAE. The deviation with respect to Trouton law observed for our pure polymers is relatively reduced, considering the discrepancies reported in the literature [14].

These apparently contradictory results can be satisfactorily explained assuming the point of view of Macosko et al. [71], who consider that strain hardening is indeed linked to high relaxation times. This would be confirmed for our samples later, matching the extensional viscosity results with the relaxation time spectra of Figure 6. Low relaxation times are noticed for PBAT, conducting to strain softening. However, the relaxation time spectrum of PHAE is shifted to long times, which is the cause of strain hardening. These high relaxation times are due to the aforementioned hydrogen bonds between tertiary amines and hydroxyl groups. In fact, strain hardening has been reported in the literature for polymers which contain hydrogen bonds, such as hydrolyzed poly(butyl acrylate) [59]. According to these authors the cause of strain hardening is the increase of the relaxation time (Rouse time) promoted by hydrogen bonds.

These considerations should be taken into account to explain the transient extensional viscosity results of the blends (Figure 10). The blends rich in PHAE (50 PBAT/50 PHAE and 25 PBAT/75 PHAE) exhibit strain hardening behaviour, due to the hydrogen bonds between tertiary amines and hydroxyl groups of PHAE and carboxyl groups of PBAT, whereas the blend rich in PBAT, 75 PBAT/25 PHAE, shows strain softening. This agrees with the analysis of the time relaxation spectra, since the blends rich in PHAE show long relaxation times. Interestingly, when data obtained for the different strain rates are analysed it can be seen that 50 PBAT/50 PHAE shows strain hardening at the lowest extensional rate, 0.03 1/s (see Figure S5 in Supplementary Information), which is not the case of 25 PBAT/75 PHAE. Therefore, besides of the effect of hydrogen bonds, which enlarge the relaxation times, there is an effect of the morphology, currently unexplained. Actually, very few papers refer to the study of strain hardening in immiscible polymer blends [14, 21, 72] and to the eventual effect of the droplets size and interfacial tension. According to the

scarce results reported in the literature [14], the extensional viscosity is governed by the matrix. Interestingly, Al Itry et al. [21] found that the extensional viscosity increases when a compatibilizer is incorporated, due to the enhancement of the interface. In general according to the data in literature the matrix governs the extensional behaviour of the system [14]. Some authors have reported that in the case of blends of linear polymers, using compabilizer which results in an increase of the extensional viscosity [21].

Extensional viscosity results are also relevant for industrial processing, in particular for blown film extrusion. It is known that strain hardening favours considerably this process, because, the polymer melt extrudate should be stretched vertically before blowing and an increase of the viscosity with time avoids extrudate breaking. From our results of Figure 10 it can be stated that pure PBAT and 75 PBAT/25 PHAE blend could not be suitable for blown film extrusion, because they show a low elongational viscosity and no strain hardening behaviour. Our statement is supported by the results obtained by R. Al-Itry et al. [21] for a PBAT (Ecoflex FBX 7011) of the same Melt Flow Rate as the PBAT investigated in our work. The authors reported that at 180 ºC the PBAT is not apt for the blown film process, which was explained by their poor elongational properties in the molten state. Our results, as well as those of R. Al Itry et al. [21], are rather contradictory with the product information supplied by BASF that indicates that both, PBAT (Ecoflex F Blend C1200) and PBAT (Ecoflex FBX 7011), show good conditions for blown film extrusion. Under the requisites established in our laboratory and in literature [21], the ability of PBAT to be blown is questioned. But, certainly, industrial appropriate conditions, not disclosed by BASF in the Material Property Data sheet, can lead to successful blown film process of amorphous PBAT samples at considerably lower temperatures.

As compared to pure PBAT and 75 PBAT/25 PHAE, the rest of the samples are better candidates for more facile blown film extrusion, in view of the elongational flow results. In particular, pure PHAE and the blends rich in this polymer show strain hardening and a higher extensional viscosity than the other samples, which bring about advantages for processing methods involving stretching.

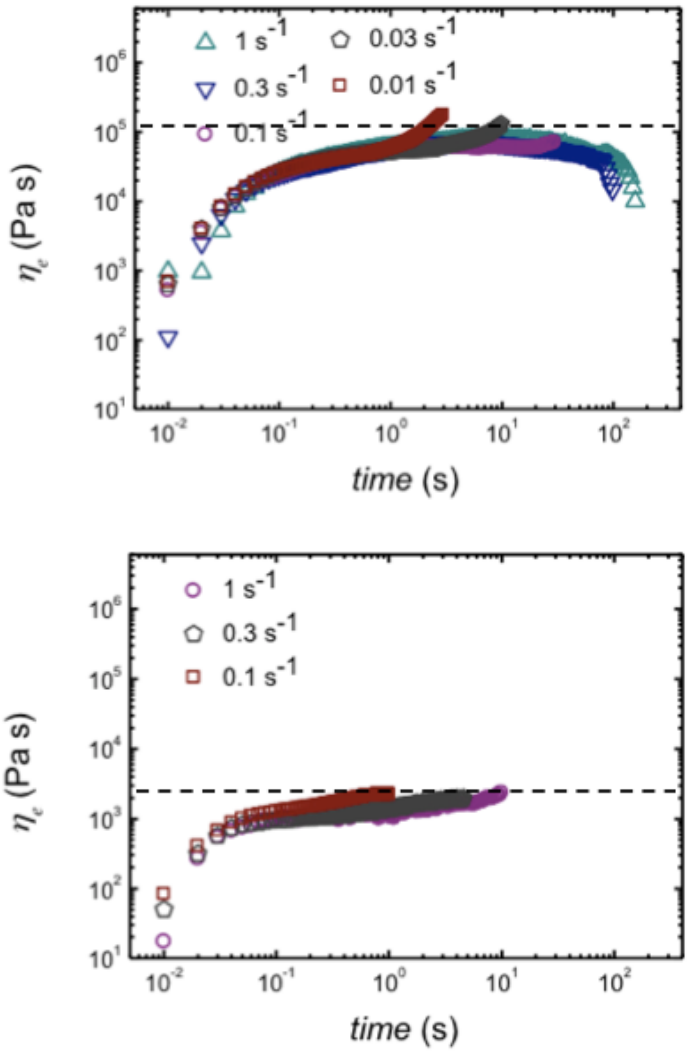

Figure 9. Extensional viscosity at different extensional rates and at 150 ºC for PHAE on the top and PBAT on the bottom. The horizontal line corresponds to the value obtained employing Trouton law $\eta_e=3\eta_o$.

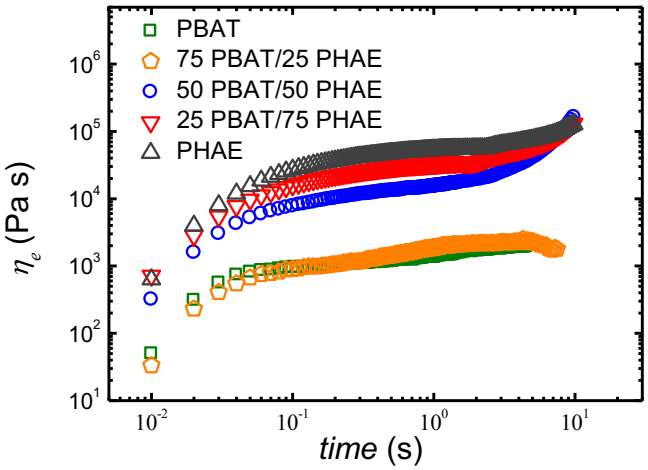

Figure 10. Extensional viscosity for the different systems studied at 0.1 s^{-1} extensional rate and 150 ºC.

Mechanical properties

In order to analyse the suitability of these blends on packaging the mechanical performance is studied. Mechanical properties of PBAT/PHAE blends and the pure components were analysed by means of tensile tests. Figure 11 shows the obtained stress-strain curves and Figures 12 (a) and (b) the values of the Young's modulus, tensile strength and ductility, measured as the elongation at break. As can be seen in both figures, PBAT exhibits the typical elastomeric behaviour of a soft material, showing low modulus (155 MPa) and tensile strength values (21.4 MPa) but a high ductility level (close to 400 %). On the contrary, the behaviour of PHAE corresponds to a stiff and brittle polymer, showing high modulus (2830 MPa), intermediate tensile strength (43.5 MPa) and low ductility values (3.5 %).

With respect to the blends, Figures 12 (a) and (b) show that Young's modulus and tensile strength exhibit a clear matrix-dependant behaviour, i.e. the 75 PBAT/25 PHAE and 50 PBAT/50 PHAE compositions shows values close to those of neat PBAT, which has been shown to be the continuous phase at these mixtures. The 25 PBAT/75 PHAE composition shows values close to those of neat PHAE, which is the matrix at this blend. This behaviour gives rise to a sigmoidal-shaped curve, leading to a clear negative deviation from the linear rule of mixtures in the PBAT-rich compositions and a slight positive deviation in the PHAE-rich composition, as can be seen in Figures 12 (a) and (b). This is not the usual behaviour of immiscible polymer

blends showing good adhesion between phases, where linear or slightly synergistic behaviours are often seen [42, 73, 74], but it can be observed in immiscible systems where adhesion between phases is not good enough to enable an effective stress transfer from the dispersed to the continuous phase [13, 44]. In addition, similar behaviours between Young's modulus and tensile strength are often seen in immiscible binary systems [13, 40, 73]. With respect to the elongation at break, it can be seen in Figure 12 (b) that it drastically decreases even at the lowest PHAE content (75 PBAT/25 PHAE composition) and blends became brittle at higher PHAE contents. As previously mentioned for Young's modulus and tensile strength, this behaviour is a consequence of a non-effective stress transfer between phases, with the rigid dispersed PHAE particles acting as stress concentrators and leading to the premature fracture of the material. Although the blends show a lower elongation at break than neat PBAT, they present a better ductility than polylactic acid PLLA, which is one of the most promising biodegradable polymers. The elongation at break for PLLA films measured in our laboratory is 3.6 %, whereas 25 PBAT/75 PHAE and 50 PBAT/50 PHAE blends give values at least two times higher. For the blend containing just 25 % PHAE the elongation at break is more than ten times higher than that of PLLA, which makes this blend a good candidate to replace polylactic acid.

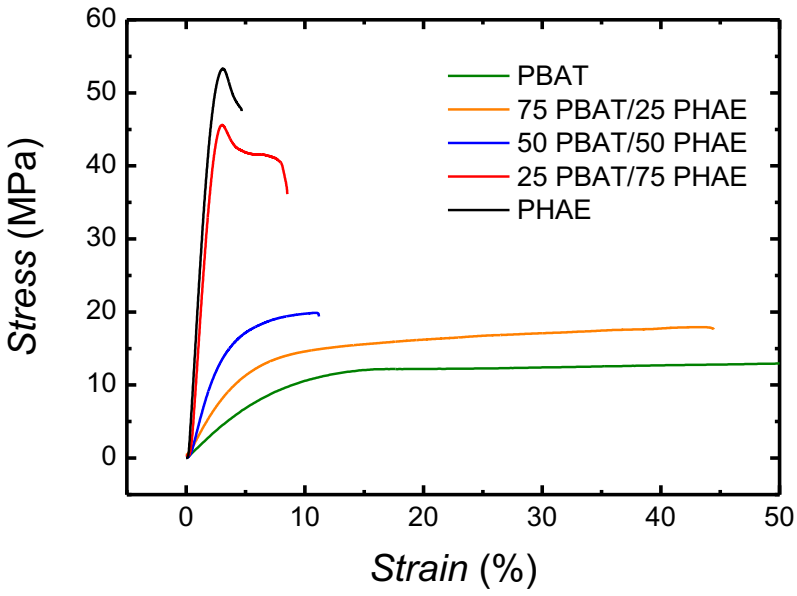

Figure 11. Stress-strain curves of pure PBAT and PHAE, and PBAT/PHAE blends. Neat PBAT elongates up to 400 %. The graph was cut in the x axis to better observe the initial part of the curves.

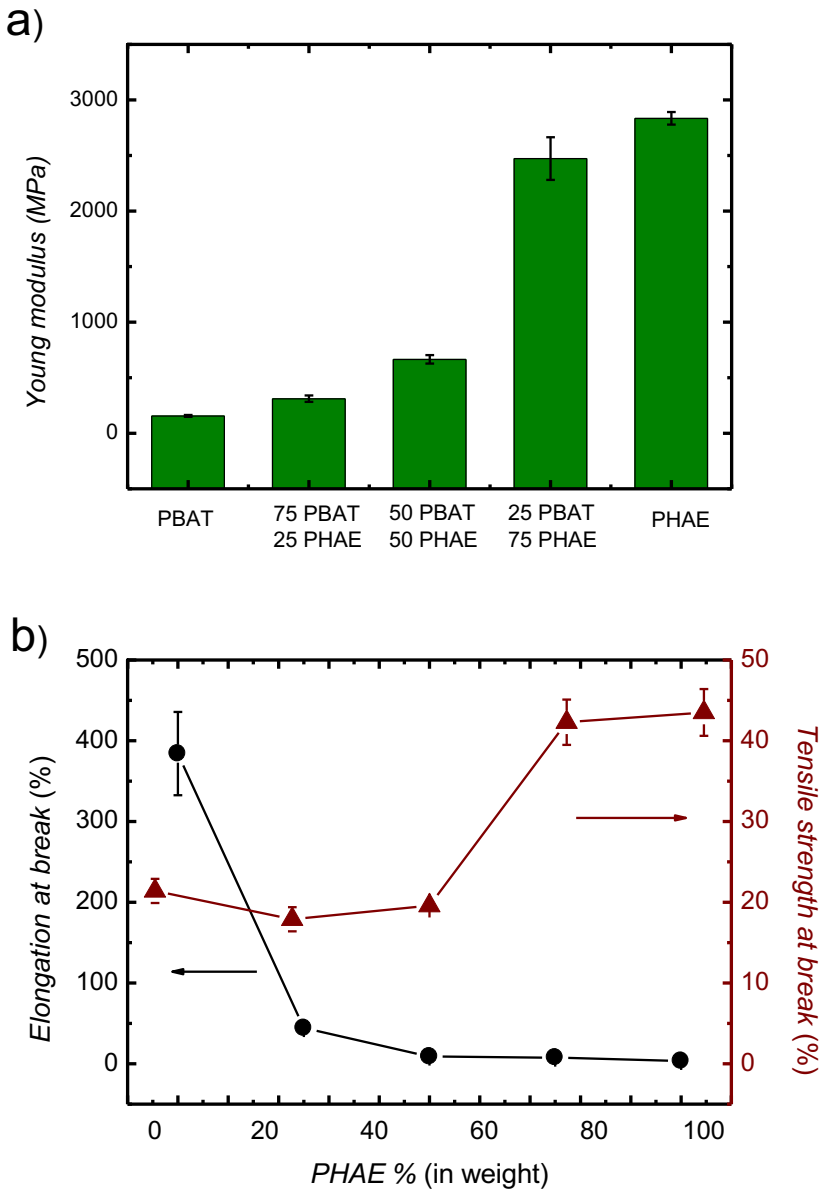

Figure 12. Young's modulus (a), tensile strength and ductility, measured as the elongation at break, (b) of pure PBAT and PHAE, and PBAT/PHAE blends.

Permeability studies

The transmission of water vapour through polymeric packaging is an important issue, since water can cause chemical and physical changes on the packaged product and it can promote the growth of microorganisms which deteriorate food [24]. On the

other hand, the permeability of polymeric packaging to aroma compounds can provide information about the loss of scent of the packed objects. In this work limonene has been used as a model compound [25] to assess the barrier features of our blends to aroma compounds.

The data obtained for water vapour transmission rate is displayed in Figure 13 and the transmission rate values are presented in Table S2. PBAT presents a high value, 12.8 g mm/m^2 day, which indicates the poor barrier character of this polymer. For biodegradable polymers lower water vapour transmission rates have been reported. For instance, 5.7 g mm/m^2 day for poly(lactide) [33], 8.6 g mm/m^2 day for poly(caprolactone) and 1.16 g mm/m^2 day for poly(hidroxybutyrate) [26]. PHAE presents a much better barrier performance than PBAT, with a value of 3.4 g mm/m^2 day. As expected, the addition of PHAE decreases considerably the permeability of PBAT to water vapour, following practically a linear decrease with the concentration of PHAE. The presence of a second phase contributes to the decrease of the permeability in two ways: Creating a tortuous pathway [75] and reducing the excess free volume, as deduced indirectly from density measurements. But, in some cases the second component can create a preferential pathway [75], which leads to obtain permeability values that are above the additive rule.

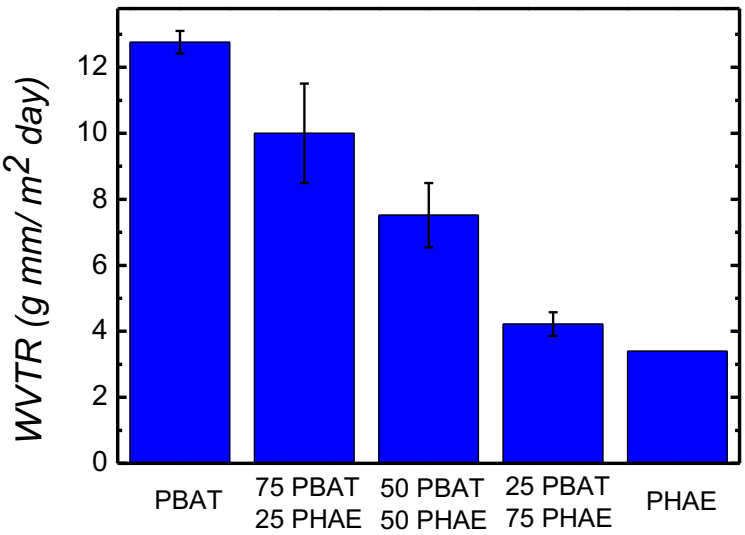

Figure 13. Water vapour transmission rate for PBAT/PHAE blends.

Several attempts have been made in literature to predict transport properties of blends [76]. In this work the most employed models have been applied: Maxwell Effective Medium Theory (EMT) and Levy [78].

Maxwell model predicts the permeability for multicomponent systems constituted by a dispersed phase and a continuous matrix. It assumes that there is no interaction between particles. A is a parameter that describes the geometry of the dispersed phase: $A = 2$ for spherical particles, $A = 1$ for transverse cylinders, $A = 0$ for planar laminar structures perpendicular to the gas flow and $A \to \infty$ when there are planar laminates parallel to the gas flow [77, 78].

$$P_{Maxwell} = P_m \frac{P_d + AP_d - A\phi\left(P_m - P_d\right)}{P_d + AP_m\phi\left(P_m P_d\right)} \tag{6}$$

where P_d and P_m are the permeability of the dispersed phase and the matrix, respectively, and ϕ is the fractional volume of the dispersed phase.

The Effective Medium Theory (EMT) does not distinguish between the dispersed phase and the matrix, which makes a good model for composition near 50 %, and there are not assumptions about geometry [79].

$$\phi \frac{P_d - P_{EMT}}{P_d + 2P_{EMT}} + (1-\phi)\frac{P_m - P_{EMT}}{P_m + 2P_{EMT}} = 0 \tag{7}$$

Levy model is the average of both Maxwell configurations and it does not distinguish between the dispersed phase and the matrix [80].

$$P_{Levy} = P_m \frac{2P_m + P_d - 2\left(P_m - P_d\right)F}{2P_m + P_d + \left(P_m - P_d\right)F} \tag{8}$$

where F and G are given by,

$$F = \frac{\frac{2}{G} - 1 + 2\phi - \sqrt{\left(\frac{2}{G} - 1 + 2\phi\right)^2 - \frac{8\phi}{G}}}{2} \tag{9}$$

$$G = \frac{\left(P_m - P_d\right)^2}{\left(P_m + P_d\right)^2 + \frac{P_m P_d}{2}} \tag{10}$$

In Figure 14 the predicted values employing different models and experimental results are shown, (see Table S3 in supplementary material for the permeability prediction values). Maxwell model was applied considering a spherical morphology, $A = 2$, and as can be seen the prediction is quite good for both compositions,

especially for 75 % PBAT. Maxwell model with A = 1 has been also applied, which is the morphology for transverse cylinders. The prediction is also good and for 25 PBAT/75 PHAE even better results than with A = 2 are obtained, although TEM micrographs show spherical droplets. In any case, the differences between the employed prediction models are very small.

Furthermore EMT model and Levy model have been applied obtaining results that overestimate and underestimate the obtained results, specially for 50 PBAT/50 PHAE underestimating the experimental results since the improvement with the addition of PHAE is lower than expected.

Overall, relatively good results are obtained with the models employed and the assumptions about the dispersed phase morphology do not have a great impact on the obtained results. It can be concluded that EMT and Levy models are more adequate for blends with similar contents of both components (50 %) since no assumptions about the dispersed phase and matrix and the geometry are made.

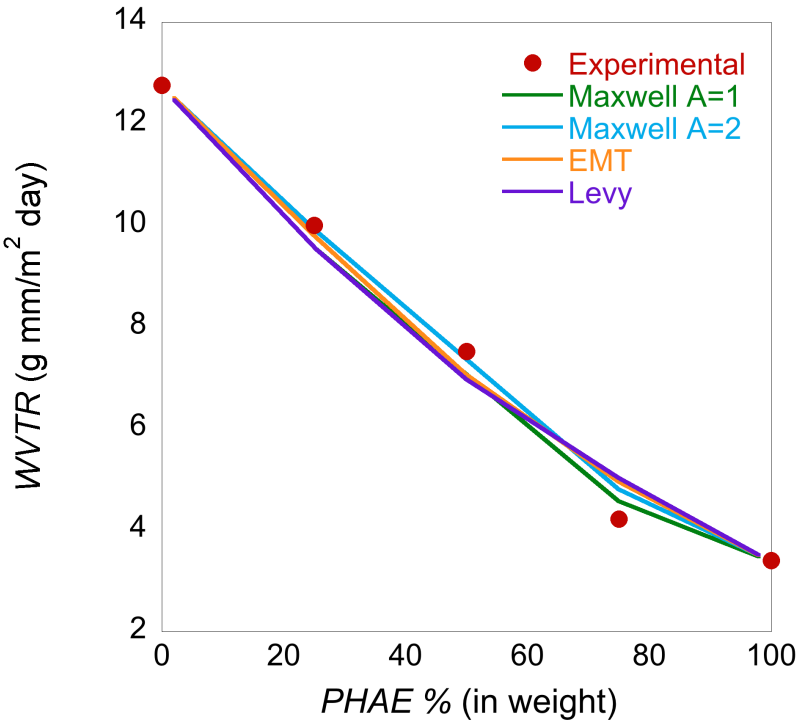

Figure 14. Experimental permeability values and theoretical predictions for water vapour transmission rate of PBAT/PHAE blends.

Regarding the transmission rate of limonene, shown in Figure 15, pure PBAT shows a value of 4.3 g mm/m^2 day and PHAE, 3.6 10^{-6} g mm/m^2 day, which corroborates the low barrier performance of PBAT and the excellent barrier character of PHAE. Taking into account the results it can be stated that the permeability to

water vapour is favoured by the hydrogen bonds and dipole-dipole interactions with the polymer. This enhances the solubility and diffusion of the penetrant, increasing the permeability. On the other hand, limonene, that is a non-polar hydrocarbon, can only form weak van der Waals bonds with the polymer which leads to lower permeability values. A similar behaviour has been observed in the literature for poly(lactide), obtaining higher values for water vapour than for limonene [81]. However, poly(caprolactone) and poly(3-hydroxybutyrate-co-3-hydroxyvalerate) show the opposite behaviour that can be attributed to the larger alkyl groups which change the nature of the interactions between polymer and penetrants [81, 82].

The permeability to limonene obtained for the blends is close to what corresponds to the additivity rule, being this behaviour the same as for water vapour.

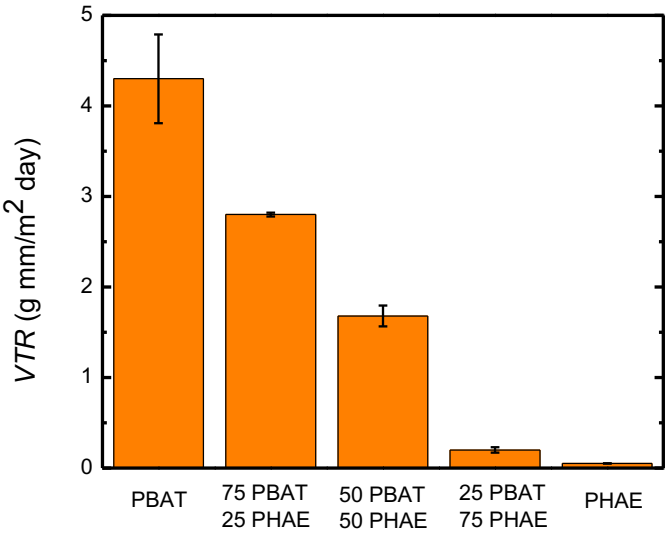

Figure 15. Limonene transmission rate for PBAT/PHAE blends.

Carbon dioxide is a penetrant of interest for food packaging application, given that is widely employed in modified atmosphere packaging (MAP) [83]. In Table 4 the carbon dioxide permeability for PBAT/PHAE bends is reported. PBAT presents a poor barrier character to this penetrant, 8.0 Barrer. Taking into account the non-polar character of CO_2, this feature can be attributed to the favoured interactions between the polymer and the penetrant, which increase solubility and diffusion and, therefore, permeability. Regarding pure PHAE, a permeability of 0.02 Barrer was calculated previously in our laboratory by sorption method and employing the well-known equation $P = D \cdot S$ [10]. Regarding solubility coefficient a value of 0.0284 (cc STP/cc pol) was reported for PHAE [10] whereas for PBAT a value of 0.0427 (cc STP/cc

pol) is obtained for the amorphous part. Therefore, it can be concluded that carbon dioxide interacts more favourably with PBAT than with PHAE.

The addition of 25 % PHAE reduces the permeability of PBAT by 86 % and with 50 % PHAE the reduction is close to 94 %. The presence of PHAE changes the transport mode of PBAT: diffusion is hindered, since the less permeating PHAE droplets increase the tortuous pathway decreasing the diffusion. On the other hand, sorption may not be greatly influenced, since PHAE phase is minority with respect to PBAT. Overall, the less favourable interactions between PHAE and CO_2, added to the increased tortuous pathway, provoke a great decrease in CO_2 permeability. Similar findings were observed for Polyamide 6/ PHAE blends [10].

Table 4. Carbon dioxide permeability of PBAT/ PHAE blends.

Sample	*P* CO_2 (Barrer)
PBAT	8.0 ± 0.02
75 PBAT/25 PHAE	1.14 ± 0.09
50 PBAT/50 PHAE	0.5 ± 0.06
25 PBAT/75 PHAE	-
PHAE	0.02

Conclusions

The analysis of the miscibility and morphological features reveals that poly(butylene adipate-co-terephthalate)/poly(hydroxyamino ether) blends are partially miscible, with a droplet/matrix morphology and good adhesion between phases. These features, together with the presence of hydrogen bonds between hydroxyl groups and tertiary amines of PHAE and carbonyl groups of PBAT, determine the linear viscoelastic properties obtained by SAOS. It is demonstrated that the blends rich in PHAE present the higher relaxation times, which in turn gives rise to a strain hardening behaviour in extensional flow. This is a relevant result, because strain hardening guarantees adequate conditions for extrusion blowing film elaboration for packaging purposes.

Taking into account the partial miscibility of the blends, the mechanical properties have been characterized where it is shown that the blends exhibit a matrix dependant behaviour. Finally the permeability to water vapour, limonene and carbon dioxide has been studied, observing an outstanding reduction with the addition of PHAE, especially for carbon dioxide. This work entitles a better understanding of the effect of a second component in the improvement of the processing and the barrier character of a biodegradable polymer, which will be beneficial for the development of bio based materials for packaging applications.

Acknowledgements

The authors are grateful to the financial support from the Basque Government (GIC IT-618-13 and GIC IT-586-13) and Spanish Ministry of Innovation and Competitiveness MINECO (MAT-2016-78527-P). A. Sangroniz and L. Sangroniz thank the Basque Government and Spanish Ministry (FPU), respectively, for their PhD grants.

References

[1] R.A. Gross, B. Kalra, Biodegradable Polymers for the Environment Green Chemistry 297 (2002) 803-807.
[2] I. Vroman, L. Tighzert, Biodegradable polymers, Materials 2 (2009) 307-344.
[3] W. Amass, A. Amass, B. Tighe, A review of biodegradable polymers: uses, current developments in the synthesis and characterization of biodegradable polyesters, blends of biodegradable polymers and recent advances in biodegradation studies, Polymer International 47 (1998) 89-144.
[4] R. Herrera, L. Franco, A. Rodríguez-Galán, J. Puiggalí, Characterization and degradation behavior of poly(butylene adipate-co-terephthalate)s, Journal of Polymer Science Part A: Polymer Chemistry 40 (2002) 4141-4157.
[5] A. Sangroniz, A. Gonzalez, L. Martin, L. Irusta, M. Iriarte, A. Etxeberria, Miscibility and degradation of polymer blends based on biodegradable poly(butylene adipate- co -terephthalate), Polymer Degradation and Stability (2018).
[6] A. Granado, J.I. Eguiazábal, J. Nazábal, Structure and properties of a poly(amino ether) resin after reprocessing in the melt state, Journal of Applied Polymer Science 101 (2006) 1368-1373.
[7] D.J. Brennan, J.E. White, A.P. Haag, S.L. Kram, M.N. Mang, S. Pikulin, C.N. Brown, Poly(hydroxy amide ethers): New High-Barrier Thermoplastics, Macromolecules 29 (1996) 3707-3716.
[8] J.E. White, H.C. Silvis, M.S. Winkler, T.W. Glass, E. Kirkpatrick, Poly(hydroxyaminoethers): a new family of epoxy-based thermoplastics, Advanced Materials 12 (2000) 1791-1800.

[9] G. Guerrica-Echevarría, J.I. Eguiazábal, J. Nazábal, Synergestic mechanical behaviour in new polyamide 6:poly(amino-ether)blends, Journal of Materials Science 37 (2002) 4529-4535.
[10] S. Eceolaza, M. Iriarte, C. Uriarte, A. Etxeberria, Barrier property enhancement of polyamide 6 by blending with a polyhydroxyamino-ether resin, Journal of Polymer Science Part B: Polymer Physics 47 (2009) 1625-1634.
[11] A. Granado, J.I. Eguiazábal, J. Nazábal, Phase behavior and mechanical properties of poly(butylene terephthalate) and poly(amino-ether) resin, Journal of Applied Polymer Science 91 (2004) 132-139.
[12] A. Granado, J.I. Eguiazábal, J. Nazábal, Preparation of Poly(ethylene terephthalate)/Poly(amino ether) Blends by means of the Addition of Poly(butylene terephthalate), Macromolecular Materials and Engineering 289 (2004) 997-1003.
[13] A. Granado, J.I. Eguiazábal, J. Nazábal, Structure and mechanical properties of blends of poly(ε - caprolactone) with a poly(amino ether), Journal of Applied Polymer Science 109 (2008) 3892-3899.
[14] L.A. Utracki, C.A. Wilkie, Polymer Blends Handbook, Springer, Netherlands, 2014.
[15] C.D. Han, Mulltiphase Flow in Polymer Processing Academic Press, New York, 1981.
[16] C.D. Han, Rheology in Polymer Processing, Academic Press, New York, 1976.
[17] L.A. Utracki, Polymer Alloys and Blends: Thermodynamics and Rheology, Hanser Publisher, New York, 1989.
[18] M. Nofar, A. Maani, H. Sojoudi, M.C. Heuzey, P.J. Carreau, Interfacial and rheological properties of PLA/PBAT and PLA/PBSA blends and their morphological stability under shear flow, Journal of Rheology 59 (2015) 317-333.
[19] R. Li, W. Yu, C. Zhou, Rheological Characterization of Droplet - Matrix versus Co - Continuous Morphology, Journal of Macromolecular Science, Part B 45 (2011) 889-898.
[20] C.R. López-Barrón, C.W. Macosko, Rheology of compatibilized immiscible blends with droplet-matrix and cocontinuous morphologies during coarsening, Journal of Rheology 58 (2014) 1935-1953.
[21] R. Al-Itry, K. Lamnawar, A. Maazouz, Biopolymer Blends Based on Poly (lactic acid): Shear and Elongation Rheology/Structure/Blowing Process Relationships, Polymers 7 (2015) 939-962.
[22] H. Eslami, M.R. Kamal, Effect of a chain extender on the rheological and mechanical properties of biodegradable poly(lactic acid)/poly[(butylene succinate)-co-adipate] blends, Journal of Applied Polymer Science 129 (2013) 2418-2428.
[23] H. Eslami, M.R. Kamal, Elongational rheology of biodegradable poly(lactic acid)/poly[(butylene succinate)-co-adipate] binary blends and poly(lactic acid)/poly[(butylene succinate)-co-adipate]/clay ternary nanocomposites, Journal of Applied Polymer Science 127 (2013) 2290-2306.
[24] V. Siracusa, P. Rocculi, S. Romani, M.D. Rosa, Biodegradable polymers for food packaging: a review, Trends in Food Science & Technology 19 (2008) 634-643.
[25] R. Auras, B. Harte, S. Selke, An overview of polylactides as packaging materials, Macromol Biosci 4 (2004) 835-64.

[26] O. Miguel, J.J. Iruin, Evaluation of the transport properties of Poly(3-hydroxybutyrate) and its 3-hydroxyvalerate copolymers for packaging applications, Macromoleculecular Symposia 144 (1999) 427-438.
[27] M.D. Sanchez-Garcia, M.J. Ocio, E. Gimenez, J.M. Lagaron, Novel Polycaprolactone Nanocomposites Containing Thymol of Interest in Antimicrobial Film and Coating Applications, Journal of Plastic Film & Sheeting 24 (2008) 239-251.
[28] M. Żenkiewicz, J. Richert, Permeability of polylactide nanocomposite films for water vapour, oxygen and carbon dioxide, Polymer Testing 27 (2008) 835-840.
[29] S.G. George, S. Thomas, Transport phenomena through polymeric systems, Progress in Polymer Science 26 (2001) 985-1017.
[30] S.Y. Lee, S.C. Kim, Laminar morphology development and oxygen permeability of LDPE/EVOH blends, Polymer Engineering & Science 37 (1997) 463-475.
[31] O. Miguel, J.J. Iruin, M.J. Fernandez-Berridi, Survey on Transport Properties of Liquids, Vapors, and Gases in Biodegradable Poly(3-hydroxybutyrate) (PHB) Journal of Applied Polymer Science 64 (1997) 1849-1859.
[32] P. Tiemblo, M.-F. Laguna, F. García, J.M. García, E. Riande, J. Gúzman, Gas Transport Properties of Poly(2-ethoxyethyl methacrylate-co-2-hydroxyethyl methacrylamide), Macromolecules 37 (2004) 4156-4163.
[33] A. Sangroniz, A. Chaos, Y.M. Garcia, J. Fernández, M. Iriarte, A. Etxeberria, Improving the barrier character of polylactide/phenoxy immiscible blend using poly(lactide-co-ε-caprolactone) block copolymer as a compatibilizer, Journal of Applied Polymer Science 134 (2017) 45396.
[34] E. Lizundia, J.L. Vilas, A. Sangroniz, A. Etxeberria, Light and gas barrier properties of PLLA/metallic nanoparticles composite films, European Polymer Journal 91 (2017) 10-20.
[35] O. Olabisi, L.M. Robeson, M.T. Shaw, Polymer-polymer miscibility, Academic Press, New York, 1979.
[36] C.C. Huang, F.C. Chang, Reactive compatibilization of polymer blends of poly(butylene terephthalate) (PBT) and polyamide-6,6 (PA66): 1. Rheological and thermal properties, Polymer 38 (1997) 2135-2141.
[37] G. Pompe, L. Häubler, W. Winter, Investigations of the Equilibrium Melting Temperature in PBT and PC/PBT Blends, Journal of Polymer Science Part B: Polymer Physics 34 (1996) 211-219.
[38] M.S. Nikolic, J. Djonlagic, Synthesis and characterization of biodegradable poly(butylene succinate-co-butylene adipate)s, Polymer Degradation and Stability 74 (2001) 263-270.
[39] Z. Qiu, C. Yan, J. Lu, W. Yang, Miscible Crystalline/Crystalline Polymer Blends of Poly(vinylidene fluoride) and Poly(butylene succinate-co-butylene adipate): Spherulitic Morphologies and Crystallization Kinetics, Macromolecules 40 (2007) 5047-5053.
[40] A. Granado, J.I. Eguiazábal, J. Nazábal, Phase behavior and mechanical properties of blends of poly(butylene terephthalate) and poly(amino-ether) resin, Journal of Applied Polymer Science 91 (2004) 132-139.
[41] S. Eceolaza, M. Iriarte, C. Uriarte, J. del Rio, A. Etxeberria, Influence of the organic compounds addition in the polymer free volume, gas sorption and diffusion, European Polymer Journal 48 (2012) 1218-1229.

[42] J.K. Kim, D.S. Jung, J. Kim, Morphology and rheological behaviour of mixtures of poly(styrene-b-ethylene-co-butylene-styrene) block copolymer and poly(2,6-dimethyl-1,4-phenylene ether), Polymer 34 (1993) 4613-4624.
[43] S.G. Lee, J.H. Lee, K.Y. Choi, J.M. Rhee, Glass transition behavior of polypropylene/polystyrene/styrene-ethylene-propylene block copolymer blends, Polymer Bulletin 40 (1998) 765-771.
[44] A. Granado, J.I. Eguiazábal, J. Nazábal, Compatibilization of PP/PAE blends by means of the addition of an ionomer, Polymer Engineering & Science 50 (2010) 1512-1519.
[45] M.M. Coleman, P.C. Painter, J.F. Graf, Specific Interactions and the Miscibility of Polymer Blends, CRC Press, Lancaster, 1995.
[46] B. Hexig, Y. He, N. Asakawa, Y. Inoue, Diphenol miscibility effect on the immiscible polyester/polyether binary blends through intermolecular hydrogen-bonding interaction, Journal of Polymer Science Part B: Polymer Physics 42 (2004) 2971-2982.
[47] J.I. Eguiazábal, J.J. Iruin, Miscibility and thermal descomposition in phenoxy/ poly(ethylene terephthalate) and phenoxy/poly(butylene terephthalate) blends, Materials Chemistry and Physics 18 (1987) 147-154.
[48] R.B. Bird, R.C. Armstrong, O. Hassager, Dynamics of Polymeric liquids: Fluid Mechanics, Wiley and sons, New York, 1987.
[49] I. Fernandez, A. Santamaria, M. E. Muñoz, P. Castell, A rheological analysis of interactions in phenoxy/organoclay nanocomposites, European Polymer Journal 43 (2007) 3171-3176.
[50] P. Pötschke, M. Abdel-Goad, I. Alig, S. Dudkin, D. Lellinger, Rheological and dielectrical characterization of melt mixed polycarbonate-multiwalled carbon nanotube composites, Polymer 45 (2004) 8863–8870.
[51] J. M. Guenet, Thermoreversible Gelation of Polymers and Biopolymers, Academic Press, New York, 1992.
[52] K. Te Nijenhuis, Thermoreversible Networks: Viscoelastic Properties and Structure of Gels, Springer, Berlin, 1997.
[53] M. S. Barral, I. Lizaso, M. E. Muñoz, A. Santamaria, Thermoreversible gels in oil/EVA systems, Rheologica Acta 40 (2001) 193-195.
[54] J.F. Palierne, Linear rheology of viscoelastic emulsions with interfacial tension, Rheologica Acta 29 (1990) 204-214.
[55] E.H. Kerner, The elastic and thermoelastic properties of composite media, Proceedings of the Physical Society, 69B, 1956, 808-813.
[56] C. Elster, J. Honerkamp, J. Weese, Using regularization methods for the determination of relaxation and retardation spectra of polymeric liquids, Rheologica Acta 30 (1991) 161-174.
[57] J. Honerkamp, J. Weese, A nonlinear regularization method for the calculation of relaxation spectra, Rheologica Acta 32 (1993) 65-73.
[58] R. Stadler, L. de Lucca Freitas, Thermoplastic elastomers by hydrogen bonding 1. Rheological properties of modified polybutadiene, Colloid & Polymer Science 264 (1986) 773-778.
[59] A. Shabbir, H. Goldansaz, O. Hassager, E. van Ruymbeke, N.J. Alvarez, Effect of Hydrogen Bonding on Linear and Nonlinear Rheology of Entangled Polymer Melts, Macromolecules 48 (2015) 5988-5996.

[60] P.S. Calvão, M. Yee, N.R. Demarquette, Effect of composition on the linear viscoelastic behavior and morphology of PMMA/PS and PMMA/PP blends, Polymer 46(8) (2005) 2610-2620.
[61] N. Robledo, J.F. Vega, J. Nieto, J. Martínez-Salazar, The role of the interface in melt linear viscoelastic properties of LLDPE/LDPE blends: Effect of the molecular architecture of the matrix, Journal of Applied Polymer Science 114 (2009) 420-429.
[62] Y. Fang, P.J. Carreau, P.G. Lafleur, Thermal and rheological properties of mLLDPE/LDPE blends, Polymer Engineering & Science 45 (2005) 1254-1264.
[63] P. Cox, E.H. Merz, Correlation of dynamic and steady flow viscosities, Journal of Polymer Science 28, (1958) 619-622.
[64] H.C. Booij, J.H.M. Palmen, Some aspects of linear and nonlinear viscoelastic behaviour of polymer melts in shear, Rheologica Acta 21 (1982) 376-387.
[65] H.C. Booij, J.H.M. Palmen, Linear viscoelastic properties of a miscible polymer blend system, in: P. Moldenaers, R. Keunings (Eds.) Theoretical and Applied Rheology: Proceedings of the XIth International Congress on Rheology, Elsevier, Brussels, 1992, pp. 321-323.
[66] H. Mavridis, R.N. Shroff, Temperature dependence of polyolefin melt rheology, Polymer Engineering & Science 32 (1992) 17778-1791.
[67] L. Sangroniz, M.A. Moncerrate, V.A. De Amicis, J.K. Palacios, M. Fernández, A. Santamaria, J.J. Sánchez, F. Laoutid, P. Dubois, A.J. Müller, The outstanding ability of nanosilica to stabilize dispersions of Nylon 6 droplets in a polypropylene matrix, Journal of Polymer Science Part B: Polymer Physics 53 (2015) 1567-1579.
[68] L. Sangroniz, J.K. Palacios, M. Fernández, J.I. Eguiazabal, A. Santamaria, A.J. Müller, Linear and non-linear rheological behavior of polypropylene/polyamide blends modified with a compatibilizer agent and nanosilica and its relationship with the morphology, European Polymer Journal 83 (2016) 10-21.
[69] H. Münstedt, Dependence of the Elongational Behavior of Polystyrene Melts on Molecular Weight and Molecular Weight Distribution, Journal of Rheology 24 (1980) 847-867.
[70] F.J. Stadler, J. Kaschta, H. Münstedt, F. Becker, M. Buback, Influence of molar mass distribution and long-chain branching on strain hardening of low density polyethylene, Rheologica Acta 48 (2008) 479-490.
[71] L.J. Kasehagen, C.W. Macosko, Nonlinear shear and extensional rheology of long-chain randomly branched polybutadiene, Journal of Rheology 42 (1998) 1303-1327.
[72] L. Li, T. Masuda, M. Takahashi, Elongation flow behaviour of ABS polymer melts, Journal of Rheology 34 (1990) 103-116.
[73] A. Granado, J.I. Eguiazabal, J. Nazabal, High Compatibility and Improved Barrier Performance in Blends Based on a Copolyester Modified with a Poly(amino ether) Resin, Macromolecular Materials and Engineering 291 (2006) 1074-1082.
[74] A. Granado, J.I. Eguiazábal, J. Nazábal, Solid-State Structure and Mechanical Properties of Blends of an Amorphous Polyamide and a Poly(amino-ether) Resin, Macromolecular Materials and Engineering 289 (2004) 281-287.
[75] A. García, S. Eceolaza, M. Iriarte, C. Uriarte, A. Etxeberria, Barrier character improvement of an amorphous polyamide (Trogamid) by the addition of a nanoclay, Journal of Membrane Science 301 (2007) 190-199.

[76] R.M. Barrer, Diffusion and permeation in heterogeneous media, in: J. Crank, G.S. Park (Eds.), Diffusion in Polymers, Academic Press, London and New York, 1968.
[77] E. Gonzo, M. Parentis, J. Gottifredi, Estimating models for predicting effective permeability of mixed matrix membranes, Journal of Membrane Science 277 (2006) 46-54.
[78] J.A. Alfageme, M. Iriarte, J.J. Iruin, A. Etxeberria, C. Uriarte, Water-Transport Properties in Polyetherimide Blends with a Liquid Crystal Polymer, Journal of Applied Polymer Science 73 (1998) 323-332.
[79] R. Landauer, The Electrical Resistance of Binary Metallic Mixtures, Journal of Applied Physics 23 (1952) 779.
[80] J. Wang, J.K. Carson, M.F. North, D.J. Cleland, A new approach to modelling the effective thermal conductivity of heterogeneous materials, International Journal of Heat and Mass Transfer 49 (2006) 3075-3083.
[81] M.D. Sanchez-Garcia, E. Gimenez, J.M. Lagaron, Morphology and barrier properties of nanobiocomposites of poly(3-hydroxybutyrate) and layered silicates, Journal of Applied Polymer Science 108 (2008) 2787-2801.
[82] M.D. Sanchez-Garcia, J.M. Lagaron, Novel clay-based nanobiocomposites of biopolyesters with synergistic barrier to UV light, gas, and vapour, Journal of Applied Polymer Science 118 (2010) 188-199.
[83] N. Gontard, R. Thibault, B. Cuq, S. Guilbert, Influence of relative humidity and film composition on oxygen and carbon dioxide permeabilities of edible films, Journal of agricultural and food chemistry 44 (1995) 1064-1069.